Therapeutics and Clinical Risk Management

Dovepress
Taylor & Francis Group

Open Access Full Text Article

ORIGINAL RESEARCH

Clinical and Procedural Predictive Model for Pneumothorax Risk After CT-Guided Lung Biopsy

Yongchao Qin[1], Zhenyu Zhao[2], Lele Zhang[2], Xiaonan Shao[3–5], Qianyun Wang[5,6]

[1]Department of Radiology, Western Beijing Cancer Hospital, Beijing, 100161, People's Republic of China; [2]Department of Nuclear Medicine, Nanjing First Hospital, Nanjing Medical University, Nanjing, 210006, People's Republic of China; [3]Department of Nuclear Medicine, The Third Affiliated Hospital of Soochow University, Changzhou, 213003, People's Republic of China; [4]Institute of Clinical Translation of Nuclear Medicine and Molecular Imaging, Soochow University, Changzhou, 213003, People's Republic of China; [5]Changzhou Clinical Medical Center, Changzhou, 213003, People's Republic of China; [6]Department of Thoracic Surgery, The Third Affiliated Hospital of Soochow University, Changzhou, 213003, People's Republic of China

Correspondence: Lele Zhang, Department of Nuclear Medicine, Nanjing First Hospital, Nanjing Medical University, Nanjing, 210006, People's Republic of China, Tel +86-0-18951670138, Fax +86-025-52254223, Email smilesmilezhang@163.com; Xiaonan Shao Department of Nuclear Medicine, The Third Affiliated Hospital of Soochow University, Changzhou, 213003, People's Republic of China, Tel +86-0-13776831531, Fax +86-0519-86621235, Email scorey@sina.com

Purpose: To develop and validate a model integrating clinical/imaging and procedural variables to predict pneumothorax after CT-guided percutaneous lung nodule biopsy.

Methods: We retrospectively enrolled 395 patients and split them 7:3 into training (n=276) and validation (n=119) cohorts. Variables with $P < 0.15$ in group comparisons (combined with clinical relevance) were selected as candidates and analyzed using age- and sex-adjusted univariable logistic regression. Two prespecified logistic models were fitted: a baseline model (clinical/imaging variables only) and a full model (baseline plus procedural variables). Discrimination, calibration, and clinical utility were assessed using ROC curves, calibration plots, and decision curve analysis (DCA).

Results: Pneumothorax occurred in 22.1% (training) and 22.7% (validation). The baseline model contained BMI and emphysema grade; the full model additionally included patient position (prone or lateral vs supine) and the number of needle adjustments. In training, the full model outperformed the baseline (AUC 0.722 vs 0.630; P=0.018). In validation, AUC was 0.720 vs 0.670 (P=0.307), but the difference did not reach statistical significance. Sensitivity was higher with the full model (0.667 vs 0.593). Both models showed good calibration; the full model was closer to the ideal line across predicted probabilities of 0.1–0.5. DCA indicated greater net benefit for the full model across most threshold probabilities.

Conclusion: A model combining clinical/imaging and procedural characteristics may facilitate peri-operative risk communication and support peri-procedural risk management for CT-guided lung nodule biopsy.

Keywords: CT-guided, lung nodule, percutaneous biopsy, pneumothorax, predictive model

Introduction

Lung cancer is the leading cause of cancer-related mortality in China, and screening plays a critical role in the early detection of cancer and precancerous lesions.[1,2] In recent years, with the widespread implementation of low-dose chest CT screening, the detection rate of pulmonary nodules has increased substantially.[3,4] Although most pulmonary nodules are benign, a subset may represent early manifestations of lung cancer. Therefore, early identification and characterization of nodules are crucial for clinical decision-making.[5] CT-guided percutaneous lung nodule biopsy is an essential diagnostic approach for determining the nature of pulmonary nodules, enabling both histological and molecular analysis of lung lesions.[6] Owing to its advantages—including only local anesthesia, minimal invasiveness, relatively low cost, and high diagnostic accuracy—this technique has been widely applied in clinical practice.[7]

Although CT-guided percutaneous lung biopsy is considered a minimally invasive procedure, it can still result in various complications, including pneumothorax, hemothorax, hemoptysis, and air embolism.[8] Previous studies have shown that pneumothorax is the most common complication of this procedure, with a relatively high incidence that varies

https://doi.org/10.2147/TCRM.S579698
Received: 6 November 2025
Accepted: 27 January 2026
Published: 5 February 2026

considerably across studies. Depending on the study population, the reported incidence of pneumothorax ranges from 19% to 60%,[7,9,10] while symptomatic pneumothorax requiring chest tube drainage is 6%–18%.[11] Although pneumothorax itself is not usually a severe complication, it can lead to dyspnea, chest pain, and, in some cases, life-threatening conditions. It also prolongs hospitalization and increases the economic burden on patients.[12,13] Therefore, accurate preoperative assessment of pneumothorax risk and the implementation of effective preventive measures are essential to improving the safety of lung biopsy procedures.

Studies have confirmed that the occurrence of pneumothorax depends on multiple factors, including lesion size and depth, lesion location, radiological characteristics, the presence of emphysema, the number of pleural punctures, needle type, and the operator's level of technical expertise.[10,14,15] Puncture-related procedural parameters may increase the risk of pneumothorax by exacerbating mechanical injury to the pleura/lung parenchyma and triggering gas leakage. However, existing risk assessment tools rely on single risk factors or subjective judgment.[10,16] Although some studies have developed predictive models, these have primarily been based on clinical variables, with limited integration and comprehensive evaluation of quantifiable procedural parameters (such as patient positioning, procedure time, number of needle adjustments, parameters related to the puncture pathway, etc). Moreover, such models generally lack rigorous clinical validation, which restricts their practical utility.[17,18] Inaccurate pneumothorax risk assessment may lead to bidirectional adverse consequences. Underestimation of risk can result in inadequate preoperative preparation and insufficient postoperative surveillance, thereby delaying the recognition and management of pneumothorax. Overestimation of risk, conversely, may trigger overtreatment and excessive resource utilization, and may influence patients' willingness to undergo biopsy. Therefore, there is an urgent need to develop a well-calibrated, individualized risk prediction tool. On this basis, the present study aimed to develop and validate a multivariable predictive model for pneumothorax risk following CT-guided percutaneous lung nodule biopsy by integrating patient clinical features, imaging parameters, and procedural factors. Meanwhile, we will explore the feasibility of leveraging intra-procedural, real-time operational data to dynamically update individualized risk estimates, thereby providing more precise risk stratification and support for perioperative management in clinical practice.

Materials and Methods

Clinical Data

This was a single-center retrospective cohort study. Clinical records of 463 patients who underwent CT-guided percutaneous lung biopsy in the Department of Nuclear Medicine, Nanjing First Hospital, between January 2022 and July 2023 were reviewed. Inclusion criteria: (1) age ≥18 years; (2) chest CT showing solid or subsolid pulmonary lesions requiring further histological or cytological diagnosis; (3) CT-guided percutaneous lung biopsy performed at our institution with complete clinical, imaging, and procedural records available. Exclusion criteria: (1) severe coagulation disorders (international normalized ratio of prothrombin time >1.5 or platelet count $<50 \times 10^9$/L); (2) history of major thoracic surgery or local interventional therapy affecting lesion assessment (eg, radiofrequency ablation, brachytherapy); (3) uncontrolled acute pulmonary infection. Demographic information, imaging features, and procedural factors were collected for all eligible patients. This retrospective study used anonymized data and was approved by the institutional ethics committee [ethics number: YKK22100]; the requirement for informed consent was waived. Based on the above criteria, 395 patients were finally included (study flowchart shown in Figure 1). Patients were stratified according to outcome (occurrence of pneumothorax) and randomly assigned to the training set (n = 276) or validation set (n = 119) in a 7:3 ratio, ensuring comparable outcome distribution and minimizing sampling bias.

CT-Guided Biopsy Procedure

All percutaneous lung biopsies in this study were performed in our hospital's Department of Interventional Radiology. The primary equipment used was a Siemens Somatom Definition AS 64-slice CT scanner. Standard scanning parameters included a slice thickness and interslice gap of 5.0 mm, tube voltage of 120 kVp, and tube current–time product of 100 mAs. Intermittent CT scans were performed during critical steps such as lesion localization and needle insertion to monitor the needle tip position and ensure procedural safety.

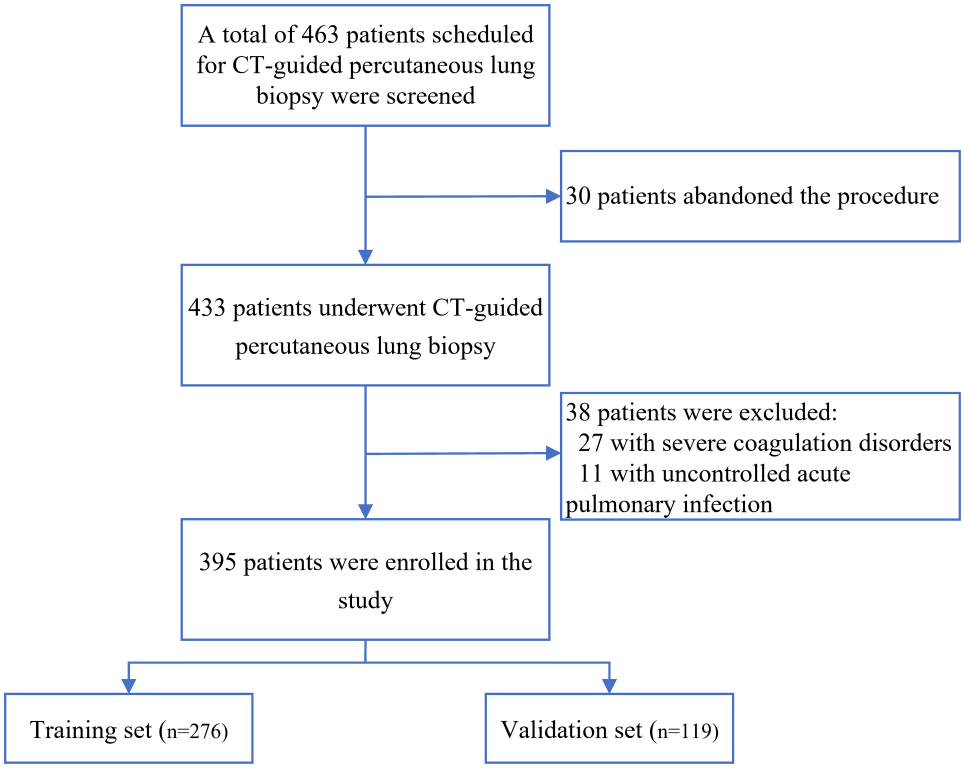

Figure 1 Study Flowchart.

Preoperative assessment of procedural risk and feasibility was conducted based on chest CT findings and the patient's clinical condition. The patient's position (supine, prone, or lateral) was selected according to the location of the lesion and the optimal access route. An initial localization scan was performed to determine the best skin entry point and puncture trajectory, which was then marked on the body surface. After routine skin disinfection and draping, local infiltration anesthesia (2% lidocaine or equivalent) was administered. All procedures used disposable coaxial cutting biopsy needles (17G coaxial system). Under CT guidance, the needle was advanced step by step, with minor angular adjustments made when necessary. Once the needle tip reached the target lesion, tissue sampling was performed.

Tissue samples were immediately submitted for pathological examination, with rapid frozen section or molecular pathology testing performed when clinically indicated. After the procedure, patients were observed supine for at least 2 hours, during which a follow-up CT or chest X-ray was performed to assess potential complications. If pneumothorax, hemorrhage, or other complications occurred, appropriate management was provided according to severity (eg, chest tube drainage, low-flow oxygen therapy). A dedicated interventional team performed all procedures to ensure sampling accuracy and procedural safety.

Data Collection

General information: Sex, age, height, weight, smoking history, and body mass index (BMI = weight [kg]/height [m]^2) were recorded.

Imaging characteristics: Preoperative chest CT was used to assess and record lesion size (maximum long-axis and short-axis diameters), lesion type (solid or subsolid), and lesion location (upper, middle, or lower lobe). Emphysema was graded based on the extent of low-attenuation areas and alveolar destruction (none, mild, or moderate–severe). The presence of bullae was also documented.

Procedural factors: These included patient position during biopsy (supine, prone, or lateral), total procedure duration (from skin disinfection and draping to needle withdrawal, in minutes), and needle insertion angle (angle between the needle and the tangent of the chest wall, in degrees). In addition, the distance traversed through lung parenchyma (from

the visceral pleura to the outer margin of the lesion along the final puncture trajectory, in mm) and the number of needle adjustments (cumulative count of intraoperative fine adjustments or reinsertion) were recorded, along with the number of biopsy cores obtained.

Outcome measures: The primary outcome was the occurrence of pneumothorax (yes/no), determined based on immediate or short-term postoperative chest CT or X-ray findings combined with clinical manifestations. Whether chest tube drainage or other interventions were performed was also documented when applicable.

Statistical Analysis

All analyses were performed using R software (version 4.2.0; http://www.R-project.org/). Continuous variables were expressed as mean ± standard deviation or median (interquartile range) and compared between groups using the independent-samples t test or Mann–Whitney U-test, as appropriate. Categorical variables were expressed as frequencies (%) and compared using the χ^2 or Fisher's exact test. Based on group comparisons in the training set, variables with $P < 0.15$ (combined with clinical relevance) were selected as candidate predictors. We intentionally applied a relatively liberal screening threshold at the univariable stage (instead of $P < 0.05$) to reduce the risk of prematurely excluding potentially important predictors in multivariable logistic regression, consistent with the purposeful selection approach.[19] Each candidate variable was then subjected to age- and sex-adjusted univariable logistic regression, with reported odds ratios (ORs) and 95% confidence intervals (CIs). Multicollinearity among candidate predictors was assessed using the variance inflation factor (VIF) prior to multivariable modeling. Variables showing substantial collinearity (VIF > 5) were not retained simultaneously, and predictors were selected to achieve model parsimony and clinical interpretability. Subsequently, two binary logistic regression models were prespecified and fitted: a baseline model (including only clinical/imaging variables) and a full model (baseline model plus procedural variables). Coefficients were estimated using maximum likelihood in the training set, without penalization or resampling. Model discrimination was evaluated using the area under the receiver operating characteristic (ROC) curve (AUC and 95% CI), and differences in AUC between models were compared using the DeLong test. For each model, an optimal probability cutoff was determined in the training set based on the Youden index of the ROC curve and was then applied unchanged to the validation set. This cutoff was used to calculate accuracy (Acc), sensitivity (Sen), specificity (Spe), positive predictive value (PPV), and negative predictive value (NPV). Model calibration was assessed using calibration plots and quantified using the Brier score. Decision curve analysis (DCA) was applied in training and validation sets to evaluate net clinical benefit across risk thresholds. All statistical tests were two-sided; a P value < 0.05 was considered statistically significant. No missing data were present in the analytic dataset; therefore, complete-case analyses were performed without imputation.

Results

A total of 395 patients were enrolled and stratified into a training set (n = 276) and a validation set (n = 119) using a 7:3 random allocation. The two cohorts had no significant differences in baseline clinical characteristics, imaging features, or procedural parameters ($P > 0.05$ for all; Supplementary Table S1). The incidence of pneumothorax was 22.1% in the training set and 22.7% in the validation set.

Comparison and Regression Analysis in the Training Set

In the training set, no significant differences were observed between the pneumothorax and non-pneumothorax groups with respect to age, sex, smoking history, height, weight, BMI, lesion size (maximum long- and short-axis diameters), lesion type (solid vs subsolid), or lesion location (upper, middle, or lower lobe) ($P > 0.05$ for all). However, the pneumothorax group had a significantly higher proportion of patients with moderate–severe emphysema (14.8% vs 5.1%, $P = 0.004$). Among procedural factors, patients in the pneumothorax group were more frequently in the supine position (59.0% vs 41.4%, $P = 0.047$), and had longer procedure times, longer intrapulmonary needle paths, and a greater number of needle adjustments (all $P < 0.05$). Regarding pathological outcomes, the pneumothorax group yielded fewer biopsy cores ($P = 0.017$), although the distribution of benign versus malignant diagnoses did not differ significantly between groups ($P > 0.05$) (see Table 1). Comparison information for the validation set can be found in Supplementary Table S2.

Table 1 Comparison of Baseline Characteristics Between Patients With and Without Pneumothorax in the Training Set

Variable	No Pneumothorax (n=215)	Pneumothorax (n=61)	P-Value
Age (years)	65.2 (11.9)	65.8 (11.3)	0.741
Gender			0.913
Female	97 (45.1%)	28 (45.9%)	
Male	118 (54.9%)	33 (54.1%)	
Smoking history	81 (37.7%)	21 (34.4%)	0.643
Height (cm)	166.3 (8.1)	166.6 (7.3)	0.782
Weight (kg)	67.7 (11.7)	65.1 (10.8)	0.121
BMI (kg/m^2)	24.4 (3.3)	23.5 (3.6)	0.055
Emphysema			0.004
No	178 (82.8%)	39 (63.9%)	
Mild	26 (12.1%)	13 (21.3%)	
Moderate-Severe	11 (5.1%)	9 (14.8%)	
Pulmonary bullae	5 (2.3%)	2 (3.3%)	0.652
Lesion type			0.749
Solid	206 (95.8%)	59 (96.7%)	
Subsolid	9 (4.2%)	2 (3.3%)	
Lesion location			0.295
Upper lobe	118 (54.9%)	33 (54.1%)	
Middle lobe	10 (4.7%)	6 (9.8%)	
Lower lobe	87 (40.5%)	22 (36.1%)	
Maximum long diameter (mm)	30.8 (21.1–44.4)	29.0 (22.3–38.7)	0.579
Maximum short diameter (mm)	24.1 (15.4–35.0)	22.8 (18.8–29.1)	0.557
Procedural factors			
Patient position			0.047
Supine	89 (41.4%)	36 (59.0%)	
Prone	112 (52.1%)	23 (37.7%)	
Lateral	14 (6.5%)	2 (3.3%)	
Procedure time (min)	28.0 (9.8)	34.4 (11.9)	<0.001
Needle angle (°)	67.6 (15.3)	68.2 (15.9)	0.802
Needle path length (mm)	24.1 (11.3–36.8)	31.6 (18.8–49.1)	0.003
Number of needle adjustments	4.0 (3.0–6.0)	5.0 (4.0–8.0)	0.002
Number of biopsy cores	3.0 (2.0–3.0)	2.0 (2.0–3.0)	0.017
Pathological diagnosis			0.985
Benign	28 (13.0%)	8 (13.1%)	
Malignant	187 (87.0%)	53 (86.9%)	

Notes: Results are presented as mean (SD), median (Q1–Q3), or n (%), as appropriate.

In age- and sex-adjusted univariable logistic regression analyses (see Table 2), BMI was identified as a protective factor (OR = 0.911, P = 0.013). Compared with patients without emphysema, the risk of pneumothorax increased in a graded manner among those with mild and moderate–severe emphysema (OR = 3.084 and 4.652, respectively; both P < 0.05). With supine position as the reference, prone positioning was associated with a lower risk of pneumothorax (OR = 0.574, P = 0.028), whereas the lateral position showed no significant difference (P = 0.445). Among continuous variables, longer procedure time, greater intrapulmonary needle path length, and more needle adjustments were all significantly associated with an increased risk of pneumothorax (OR = 1.055, 1.018, and 1.247, respectively; all P < 0.05).

Construction of the Multivariable Predictive Model

Based on the age- and sex-adjusted univariable logistic regression results (Table 2), a baseline model including only clinical and imaging variables was first established as follows:

Table 2 Univariable Logistic Regression Analysis in the Training Set (Adjusted for Age and Sex)

	Descriptive Statistics	OR (95% CI)	P-Value
Weight (kg)	67.2 (11.5)	0.978 (0.955, 1.001)	0.065
BMI (kg/m^2)	24.2 (3.4)	0.911 (0.845, 0.981)	0.013
Emphysema			
None	217 (78.6%)	1.0	
Mild	39 (14.1%)	3.084 (1.515, 6.280)	0.002
Moderate-Severe	20 (7.2%)	4.652 (2.017, 10.730)	<0.001
Patient position			
Supine	125 (45.3%)	1.0	
Prone	135 (48.9%)	0.574 (0.350, 0.940)	0.028
Lateral	16 (5.8%)	0.666 (0.235, 1.891)	0.445
Procedure time (min)	29.4 (10.7)	1.055 (1.033, 1.079)	<0.001
Needle path length (mm)	26.1 (12.7–41.1)	1.018 (1.007, 1.030)	0.002
Number of needle adjustments	5.0 (3.0–6.0)	1.247 (1.130, 1.377)	<0.001

Notes: Results are presented as mean (SD), median (Q1–Q3), or n (%), as appropriate.

Logit(P) = 0.02684 − 0.06357×BMI + 0.73206×(Emphysema=mild) + 1.22198×(Emphysema=moderate-severe), where P represents the probability of pneumothorax occurrence, with "no emphysema" used as the reference category.

Subsequently, procedural variables were added to construct a full model based on the baseline model:

Logit(P) = −0.41019 − 0.09530×BMI + 0.91479×(Emphysema =mild) + 1.65781×(Emphysema=moderate-evere) − 0.65712×(Position=Prone) − 1.18737×(Position=Lateral) + 0.27277×Number of needle adjustments, where P denotes the probability of pneumothorax, with "no emphysema" and "supine position" serving as reference categories. After multivariable adjustment, procedure time and intrapulmonary needle path length were not retained in the final model.

ROC curves were plotted for both the baseline and full models in the training and validation sets (see Figure 2A and B), and model performance metrics are summarized in Table 3. According to the DeLong test, the full model demonstrated a significantly higher AUC in the training set than the baseline model (0.722 vs 0.630, P = 0.018). In the validation set, the AUC of the full model was also higher than that of the baseline model (0.720 vs 0.670), though the difference did not reach statistical significance (P = 0.307). Notably, the full model exhibited higher sensitivity (0.667 vs 0.593), indicating a lower likelihood of missing pneumothorax cases. Regarding calibration (see Figure 2C and D), both models agreed with the ideal line in the training and validation sets. The baseline model deviated around the 0.2–0.3 predicted probability range, whereas the full model demonstrated closer alignment with the ideal line across the 0.1–0.5 range. Consistent with this visual assessment, the Brier scores were 0.164 (baseline) and 0.147 (full) in the training set, and 0.163 (baseline) and 0.160 (full) in the validation set, indicating slightly lower overall prediction error for the full model. DCA showed that the full model yielded a higher net benefit than the baseline model across a range of threshold probabilities in the validation set (see Figure 2E and F). To enhance interpretability and facilitate bedside application, nomograms for both models were constructed (see Figure 3A and B).

Discussion

This study developed a predictive model for pneumothorax following CT-guided percutaneous lung nodule biopsy using a training set and independently evaluated it in a validation set. A baseline model incorporating only clinical and imaging variables was first constructed, followed by a full model that included procedural variables. The full model demonstrated significantly better discrimination than the baseline model in the training set (AUC: 0.722 vs 0.630, DeLong P = 0.018). In the validation set, the full model also showed higher AUC and sensitivity (0.720 vs 0.670; 0.667 vs 0.593). However, the difference in AUC did not reach statistical significance (DeLong P = 0.307). DCA suggested a potentially higher net benefit of the full model across clinically relevant threshold probabilities. However, given the modest discrimination and the lack of external validation, these findings should be interpreted cautiously and viewed as hypothesis-generating.

The incidence of pneumothorax in this study was 22.1% in the training set and 22.7% in the validation set, consistent with previously reported rates.[10,20–23] A notable finding was that patients with lower BMI had a significantly higher risk

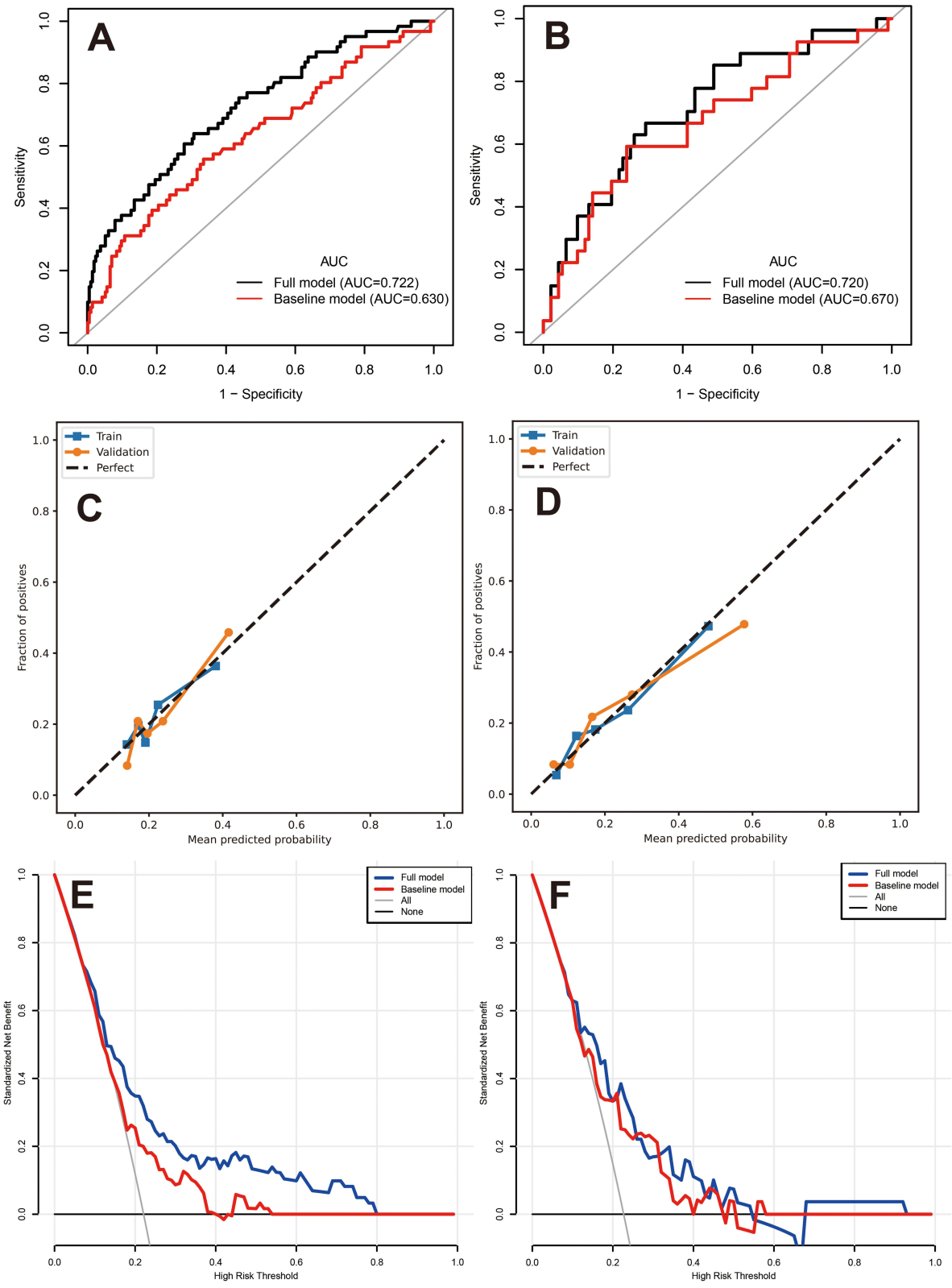

Figure 2 Comparison of the performance of the baseline and full models in the training and validation sets. (**A**) ROC curves in the training set. (**B**) ROC curves in the validation set. Black line, full mo red line, baseline mo gray diagonal line, reference (no-discrimination). (**C** and **D**) Calibration plots for the baseline model (**C**) and full model (**D**) in the training (blue) and validation (Orange) sets; the dashed line indicates perfect calibration (y = x). (**E** and **F**) Decision curve analysis (DCA) in the training (**E**) and validation (**F**) sets; blue line, full mo red line, baseline mo gray and black lines represent the treat-all and treat-none strategies, respectively. The x-axis shows threshold probability (high-risk threshold) and the y-axis shows standardized net benefit.

https://doi.org/10.2147/TCRM.S579698

Table 3 Comparison of Predictive Performance Between the Baseline and Full Models in the Training and Validation Sets

	AUC (95% CI)	Acc	Sen	Spe	PPV	NPV
Training set						
Baseline model	0.630 (0.547, 0.713)	0.641	0.557	0.665	0.321	0.841
Full model	0.722 (0.649, 0.796)	0.681	0.639	0.693	0.371	0.871
Validation set						
Baseline model	0.670 (0.548, 0.793)	0.597	0.593	0.598	0.302	0.833
Full model	0.720 (0.609, 0.831)	0.689	0.667	0.696	0.391	0.877

of pneumothorax. This may be attributed to thinner chest wall adipose tissue and weaker pleural support, making the needle tract more difficult to seal after puncture, thus predisposing to air leakage. Wang et al[24] similarly reported that each unit increase in BMI was associated with a significant reduction in pneumothorax risk, consistent with our results.

Previous studies have consistently identified emphysema as an essential risk factor for pneumothorax.[10,25,26] The likely mechanism involves reduced lung tissue elasticity and difficulty in closing the needle tract, which increases the likelihood of air leakage.[27] A prospective multicenter study reported that patients with emphysema had a 2.429-fold higher risk of pneumothorax than those without emphysema; however, that study only considered the presence or absence of emphysema and did not analyze its severity.[28] In contrast, De et al[29] classified only patients with severe emphysema as emphysema-positive, grouping those with mild or moderate disease into the non-emphysema category. In the present study, the effect of emphysema severity was quantitatively assessed. Using "no emphysema" as the reference, the risk of pneumothorax increased approximately 3.1-fold in patients with mild emphysema and 4.7-fold in those with moderate–severe emphysema, showing a precise dose–response relationship. Nonetheless, some studies have not included emphysema in their analyses or have failed to identify it as a significant risk factor.[30–32] Zhang et al[33] suggested that this inconsistency may be attributed to technical aspects, as their operators deliberately avoided puncturing through emphysematous regions, thereby reducing pneumothorax incidence.

From a procedural standpoint, this study identified the supine position during biopsy as an independent risk factor for pneumothorax. In contrast, the incidence of pneumothorax was significantly lower when patients were prone or lateral. In the supine position, the lung tissue is relatively suspended, which may predispose to air leakage; this finding is consistent with several previous studies.[15,34] Drumm et al[30] similarly reported a significantly lower pneumothorax incidence in patients positioned laterally. In contrast, Wang et al[35] observed a higher pneumothorax risk in the lateral position,

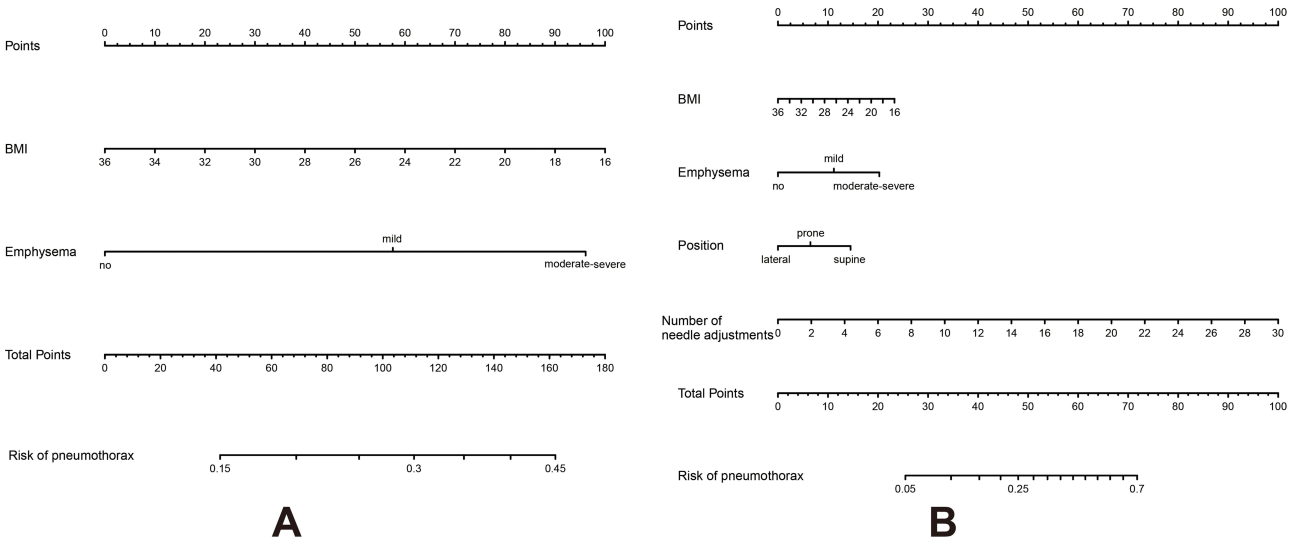

Figure 3 Nomograms of the baseline and full predictive models (**A** and **B**).

reasoning that when the biopsied lung was positioned uppermost, the separation between the parietal and visceral pleura became more pronounced, facilitating air entry into the pleural space upon needle withdrawal. Meanwhile, He et al[28] found no significant association between patient position and pneumothorax occurrence. These discrepancies may be attributable to several factors. First, study populations and lesion characteristics varied across studies (eg, the proportion of lesions located dorsally/laterally or adjacent to the pleura, as well as lesion depth and size), which may influence the optimal needle trajectory under different patient positions. Second, procedural technique and perioperative management differed, such as routine use of a coaxial needle system, needle gauge, and the number of needle passes; these factors may interact with patient positioning, resulting in inconsistency in the magnitude and direction of the positioning effect across studies. Third, differences in statistical handling and adjustment for confounding may also affect the conclusions. Therefore, the association between patient positioning and pneumothorax risk may be context dependent, and further validation under more standardized definitions of positioning and more uniform procedural protocols is warranted. Furthermore, the number of needle adjustments was also identified as an independent risk factor for pneumothorax.[36] Our results demonstrate that increased needle adjustments are significantly associated with a higher risk of pneumothorax. Generally, biopsies of smaller lesions require more frequent needle adjustments, and respiratory motion adds to procedural difficulty, often necessitating multiple directional changes to reach the target lesion.[37,38] Repeated manipulation of the needle tract can cause multiple pleural injuries, thereby increasing the likelihood of pneumothorax. Consequently, minimizing the number of punctures and pleural injuries is a key strategy for reducing pneumothorax risk.[10,15,39] These findings underscore the critical impact of procedural technical parameters on pneumothorax development. Although procedure time and needle path length were associated with the occurrence of pneumothorax in univariate analysis, their independent effects diminished and failed to maintain statistical significance after being simultaneously included in the multivariate model alongside other procedural variables. Furthermore, these factors, along with indicators such as the number of needle adjustments, clinically reflect the complexity of the procedure and may exhibit some degree of information overlap. Therefore, they were not incorporated into the final model.

In both the training and validation sets, the full predictive model—constructed by integrating the above clinical and procedural factors—demonstrated numerically better predictive performance compared with the baseline model, which included only basic clinical and imaging variables. The full model also exhibited higher sensitivity, reducing the likelihood of missed pneumothorax cases. The baseline model primarily reflects the static risk profiles of patients, whereas procedural variables are more directly associated with pleural injury and the occurrence of pneumothorax. Therefore, in patients with relatively unremarkable foundational risk profiles but higher procedural complexity or greater procedural intensity, the full model may be more adept at identifying their true risk of developing pneumothorax. This finding suggests that incorporating procedural variables enables the model to reflect real-world conditions better and overcome the static limitations of purely imaging-based models. Moreover, the model showed good calibration and higher net clinical benefit, providing a quantitative basis for preoperative risk assessment and procedural optimization. The accompanying nomogram allows clinicians to intuitively quantify an individual patient's risk of post-biopsy pneumothorax, thereby supporting more precise risk management planning, patient safety, and surgical decision-making accuracy.

This study has several limitations: 1. As a retrospective analysis, potential selection bias cannot be entirely excluded. 2. The sample size of the validation set is relatively limited, which may result in insufficient statistical power for the AUC difference test. The sensitivity was 0.667, indicating that approximately one-third of pneumothorax cases might be missed; therefore, the model should not be used as the sole tool to rule out pneumothorax, and follow-up imaging and clinical monitoring remain necessary when indicated. 3. Pulmonary function parameters, lung density measurements, the exact distance between the nodule and pleura, and additional quantitative imaging metrics were not systematically included, possibly leading to omission of certain risk factors. 4. Procedural factors may still be subject to residual confounding related to operator experience and technical variation. 5. The model was validated internally; external datasets are needed to verify its robustness and applicability further. Future research should involve multicenter, large-sample, prospective studies incorporating additional potential predictors, external validation, and model updating to enhance generalizability and predictive accuracy.

In summary, this study developed and validated a pneumothorax risk prediction model composed of BMI, emphysema severity, patient position, and the number of needle adjustments. The model demonstrated acceptable discrimination

and calibration, and decision curve analysis suggested a potential clinical net benefit across a range of threshold probabilities. These findings may facilitate peri-procedural risk communication and risk management; however, before widespread implementation, further multicenter external validation is warranted, and incorporation of additional quantifiable imaging biomarkers (eg, lung density measurements, radiomics features) and larger sample sizes should be explored to improve model stability and predictive performance. Clinically, the baseline model may be used preoperatively for preliminary stratification, whereas the full model—once procedural information becomes available—may support intra-procedural risk updating and help identify patients who may benefit from heightened monitoring and preparedness for intervention. Further external validation and prospective impact studies are warranted before widespread implementation.

Data Sharing Statement

The datasets used and/or analyzed during the current study are available from the corresponding authors (Lele Zhang, smilesmilezhang@163.com; Xiaonan Shao, scorey@sina.com) upon reasonable request.

Ethics Approval and Consent to Participate

This study adhered to the principles of the Declaration of Helsinki and was approved by the Ethics Committee of Nanjing First Hospital [ethics number: YKK22100]. Since the patients were anonymized, the hospital's ethics committee waived informed consent. See Figure 1 for the enrollment flowchart.

Funding

This study was supported by Nanjing Health Science and Technology Development Special Funding Program (YKK22100); Top Talent of Changzhou "The 14th Five-Year Plan" High-Level Health Talents Training Project (2022CZBJ037); Changzhou Science and Technology Bureau (CJ20241104).

Disclosure

The authors declare that they have no competing interests relevant to the content of this article.

References

1. Sung H, Ferlay J, Siegel RL. et al. Global Cancer Statistics 2020: GLOBOCAN Estimates of Incidence and Mortality Worldwide for 36 Cancers in 185 Countries. *CA Cancer J Clin*. 2021;71(3):209–249. doi:10.3322/caac.21660
2. Xia C, Dong X, Li H, et al. Cancer statistics in China and United States, 2022: profiles, trends, and determinants. *Chin Med J*. 2022;135 (5):584–590. doi:10.1097/CM9.0000000000002108
3. Gould MK, Tang T, Liu IL, et al. Recent Trends in the Identification of Incidental Pulmonary Nodules. *Am J Respir Crit Care Med*. 2015;192 (10):1208–1214. doi:10.1164/rccm.201505-0990OC
4. Choi HK, Mazzone PJ. Lung Cancer Screening. *Med Clin North Am*. 2022;106(6):1041–1053. doi:10.1016/j.mcna.2022.07.007
5. MacMahon H, Naidich DP, Goo JM, et al. Guidelines for Management of Incidental Pulmonary Nodules Detected on CT Images: from the Fleischner Society 2017. *Radiology*. 2017;284(1):228–243. doi:10.1148/radiol.2017161659
6. Maalouf N, Abou Mrad M, Benayed R, Pugliesi RA, Apitzsch J. The Interplay of Time and Angle with the Incidence of Pneumothorax in Computed Tomography-Guided Lung Biopsy. *RoFo*. 2025;2025:1.
7. Çakir Ö, Çam I, Koç U, Çiftçi E. Evaluation of major complications associated with percutaneous CT-guided biopsy of lung nodules below 3 cm. *Turk J Med Sci*. 2020;50(2):369–374. doi:10.3906/sag-1908-73
8. Satomura H, Higashihara H, Kimura Y, et al. Normal saline injection and rapid rollover; preventive effect on incidence of pneumothorax after CT-guided lung biopsy: a retrospective cohort study. *BMC Pulm Med*. 2024;24(1):505. doi:10.1186/s12890-024-03315-z
9. Zhou SQ, Luo F, Ran X, Yang J, Lv FR, Li K. Nonlinear association between lung needle path CT attenuation values and postprocedural immediate pneumothorax following computed tomography-guided lung biopsy: a retrospective cohort study. *BMC Pulm Med*. 2024;24(1):567. doi:10.1186/s12890-024-03343-9
10. Leonhardi J, Dahms U, Schnarkowski B, et al. Impact of radiomics features, pulmonary emphysema score and muscle mass on the rate of pneumothorax and chest tube insertion in CT-guided lung biopsies. *Respir Res*. 2024;25(1):320. doi:10.1186/s12931-024-02936-6
11. Shera FA, Shera TA, Shah OA, et al. Pneumothorax after CT-Guided Lung Biopsy: what Next? *Indian J Radiol Iimag*. 2023;33(3):309–314. doi:10.1055/s-0043-1764293
12. Baumann MH, Noppen M. Pneumothorax. *Respirology*. 2004;9(2):157–164. doi:10.1111/j.1440-1843.2004.00577.x
13. Luengo-Fernandez R, Landeiro F, Hallifax R, Rahman NM. Cost-effectiveness of ambulatory care management of primary spontaneous pneumothorax: an open-label, randomised controlled trial. *Thorax*. 2022;77(9):913–918. doi:10.1136/thoraxjnl-2021-218479
14. Görgülü FF, Öksüzler FY, Arslan SA, Arslan M, I E Ö, Görgülü O. Computed tomography-guided transthoracic biopsy: factors influencing diagnostic and complication rates. *J Int Med Res*. 2017;45(2):808–815. doi:10.1177/0300060517698064

15. Ruud EA, Stavem K, Geitung JT, Borthne A, Søyseth V, Ashraf H. Predictors of pneumothorax and chest drainage after percutaneous CT-guided lung biopsy: a prospective study. *Eur Radiol*. 2021;31(6):4243–4252. doi:10.1007/s00330-020-07449-6
16. Deng XB, Xie L, Zhu HB, et al. The nodule-pleura relationship affects pneumothorax in CT-guided percutaneous transthoracic needle biopsy: avoiding to cross pleural tail sign may reduce the incidence of pneumothorax. *BMC Pulm Med*. 2024;24(1):490. doi:10.1186/s12890-024-03307-z
17. Yang L, Liang T, Du Y, et al. Nomogram model to predict pneumothorax after computed tomography-guided coaxial core needle lung biopsy. *Eur J Radiol*. 2021;140:109749. doi:10.1016/j.ejrad.2021.109749
18. Zhao Y, Wang X, Wang Y, Zhu Z. Logistic regression analysis and a risk prediction model of pneumothorax after CT-guided needle biopsy. *J Thoracic Dis*. 2017;9(11):4750–4757. doi:10.21037/jtd.2017.09.47
19. Bursac Z, Gauss CH, Williams DK, Hosmer DW. Purposeful selection of variables in logistic regression. *Source Code for Biology and Medicine*. 2008;3(1):17. doi:10.1186/1751-0473-3-17
20. Hui H, Yin HT, Wang T, Chen G. Computed tomography-guided core needle biopsy for sub-centimeter pulmonary nodules. *Polish J Cardio-Thoracic Surg*. 2022;19(2):65–69. doi:10.5114/kitp.2022.117492
21. Li Y, Wang T, Fu YF, Shi YB, Wang JY. Computed tomography-guided biopsy for sub-centimetre lung nodules: technical success and diagnostic accuracy. *Clin Respiratory J*. 2020;14(7):605–610. doi:10.1111/crj.13172
22. Portela de Oliveira E, Souza CA, Inacio JR, et al. Imaging-guided Percutaneous Biopsy of Nodules ≤1 cm: study of Diagnostic Performance and Risk Factors Associated With Biopsy Failure. *J Thoracic Imaging*. 2020;35(2):123–128. doi:10.1097/RTI.0000000000000427
23. Pugliesi RA, Nasser Y, Benchekroun A, et al. Impact of Technical Standardization on Pneumothorax and Chest Tube Insertion Rates: a Retrospective Learning Curve Analysis of CT-Guided Lung Biopsies. *J Clin Med*. 2025;14(14):4838. doi:10.3390/jcm14144838
24. Wang S, Tu J, Chen W. Development and Validation of a Prediction Pneumothorax Model in CT-Guided Transthoracic Needle Biopsy for Solitary Pulmonary Nodule. *Biomed Res Int*. 2019;2019:7857310. doi:10.1155/2019/7857310
25. Saade C, Zien-El-Dine S, Hamieh N, et al. Lung density in the trajectory path is a strong indicator of patients sustaining a pneumothorax during CT-guided lung biopsy. *Adv Rspiratory Med*. 2020;88(2):108–115. doi:10.5603/ARM.2020.0084
26. Yang X, Cheng HT, Huang Y, et al. Safety and efficacy of tract embolization using gelatin sponge particles in reducing pneumothorax after CT-guided percutaneous lung biopsy in patients with emphysema. *BMC Pulm Med*. 2024;24(1):329. doi:10.1186/s12890-024-03125-3
27. Huo YR, Chan MV, Habib AR, Lui I, Ridley L. Pneumothorax rates in CT-Guided lung biopsies: a comprehensive systematic review and meta-analysis of risk factors. *BrJ Radiol*. 2020;93(1108):20190866. doi:10.1259/bjr.20190866
28. He C, Zhao L, Yu HL, et al. Pneumothorax after percutaneous CT-guided lung nodule biopsy: a prospective, multicenter study. *Quant Imagi Med Surg*. 2024;14(1):208–218. doi:10.21037/qims-23-891
29. De Filippo M, Saba L, Silva M, et al. CT-guided biopsy of pulmonary nodules: is pulmonary hemorrhage a complication or an advantage? *Diagnostic Interventional Radiol*. 2014;20(5):421–425. doi:10.5152/dir.2014.14019
30. Drumm O, Joyce EA, de Blacam C, et al. CT-guided Lung Biopsy: effect of Biopsy-side Down Position on Pneumothorax and Chest Tube Placement. *Radiology*. 2019;292(1):190–196. doi:10.1148/radiol.2019182321
31. Shiekh Y, Haseeb WA, Feroz I, Shaheen FA, Gojwari TA, Choh NA. Evaluation of various patient-, lesion-, and procedure-related factors on the occurrence of pneumothorax as a complication of CT-guided percutaneous transthoracic needle biopsy. *Polish J Radiol*. 2019;84:e73–e79. doi:10.5114/pjr.2019.82837
32. Lee DS, Bak SH, Jeon YH, Kwon SO, Kim WJ. Perilesional emphysema as a predictor of risk of complications from computed tomography-guided transthoracic lung biopsy. *Jpn J Radiol*. 2019;37(12):808–816. doi:10.1007/s11604-019-00880-w
33. Zhang J, An J, Jing X, et al. Assessing risk factors for complications in computer tomography-guided lung biopsy: quantitative analysis for predicting pneumothorax. *Ann Saudi Med*. 2024;44(4):228–233. doi:10.5144/0256-4947.2024.228
34. Chan MV, Afraz Z, Huo YR, Kandel S, Rogalla P. Manual aspiration of a pneumothorax after CT-guided lung biopsy: outcomes and risk factors. *BrJ Radiol*. 2023;96(1148):20220366. doi:10.1259/bjr.20220366
35. Wang Y, Li W, He X, Li G, Xu L. Computed tomography-guided core needle biopsy of lung lesions: diagnostic yield and correlation between factors and complications. *Oncol Lett*. 2014;7(1):288–294. doi:10.3892/ol.2013.1680
36. Sargent T, Kolderman N, Nair GB, Jankowski M, Al-Katib S. Risk Factors for Pneumothorax Development Following CT-Guided Core Lung Nodule Biopsy. *J Bronchol Intervent Pulmonol*. 2022;29(3):198–205. doi:10.1097/LBR.0000000000000816
37. Constantinescu A, Stoicescu ER, Iacob R, et al. CT-Guided Transthoracic Core-Needle Biopsy of Pulmonary Nodules: current Practices, Efficacy, and Safety Considerations. *J Clin Med*. 2024;13(23):7330. doi:10.3390/jcm13237330
38. Nour-Eldin NE, Alsubhi M, Emam A, et al. Pneumothorax Complicating Coaxial and Non-coaxial CT-Guided Lung Biopsy: comparative Analysis of Determining Risk Factors and Management of Pneumothorax in a Retrospective Review of 650 Patients. *Cardiovascular and Interventional Radiology*. 2016;39(2):261–270. doi:10.1007/s00270-015-1167-3
39. Khan MF, Straub R, Moghaddam SR, et al. Variables affecting the risk of pneumothorax and intrapulmonal hemorrhage in CT-guided transthoracic biopsy. *Eur Radiol*. 2008;18(7):1356–1363. doi:10.1007/s00330-008-0893-1